Exact Conditional and Unconditional Cramer-Rao Bounds for Near Field Localization

Youcef Begriche, Messaoud Thameri, Karim Abed-Meraim

Exact Conditional and Unconditional Cramér-Rao Bounds for Near Field Localization

Youcef Begriche[1], Messaoud Thameri[1] and Karim Abed-Meraim[2]

Abstract

This paper considers the Cramér-Rao lower Bound (CRB) for the source localization problem in the near field. More specifically, we use the exact expression of the delay parameter for the CRB derivation and show how this 'exact CRB' can be significantly different from the one given in the literature based on an approximate time delay expression (usually considered in the Fresnel region). In addition, we consider the exact expression of the received power profile (i.e., variable gain case) which, to the best of our knowledge, has been ignored in the literature. Finally, we exploit the CRB expression to introduce the new concept of Near Field Localization Region (NFLR) for a target localization performance associated to the application at hand. We illustrate the usefulness of the proposed CRB derivation as well as the NFLR concept through numerical simulations in different scenarios.

Index Terms

Cramér-Rao Bound, Near field, Source localization, Fresnel region, Power profile.

[1] TELECOM ParisTech, TSI Department, France. e-mail:Youcef.Begriche@ieee.org

[1] TELECOM ParisTech, TSI Department, France. e-mail:thameri@telecom-paristech.fr

[2] PRISME Laboratory, Polytech'Orléans, Orléans University, France. e-mail: karim.abed-meraim@univ-orleans.fr

I. Introduction

Sources localization problem has been extensively studied in the literature but most of the research works are dedicated to the far field case, e.g., [1], [2].

In this paper, we focus on the situation where the sources are in a near field (NF) region which occurs when the source ranges to the array are not 'sufficiently large' compared with the aperture of the array system [3], [4]. Indeed, this particular case has several practical applications including speaker localization and robot navigation [5], [6], underwater source localization [7], near field antenna measurements [8], [9] and certain biomedical applications, e.g., [10]. Recently, some works considered both far filed and near filed localization [11], [12] where the authors propose different methods to achieve a better localization performance when the source moves from far field to near field and vice versa.

More specifically, this paper is dedicated to the derivation of the Cramér-Rao Bound (CRB) expressions for different signal models and their use for the better understanding of this particular localization problem. CRB derivation for the near field case has already been considered in the literature [3], [13], [14], [15]. In [3], [13], the exact expression of the time delay has been used to derive the unconditional CRB in matrix form, i.e., expressed and computed numerically as the inverse of the Fisher Information Matrix (FIM). In [14], the conditional CRB based on an approximate model (i.e., approximate time delay expression as shown in Section II-A) is provided.

Recently, El Korso et al. derived analytical expressions of the conditional and unconditional CRB for near field localization based on an approximate model [15]. In the latter work, both conditional and unconditional CRB of the angle parameter are found independent from the range value and are equal to those of far field region.

In our work, we propose first, to use the exact time delay expression as well as the exact power profile (i.e., Variable Gain (VG) model) corresponding to the spherical form of the wavefront for the derivation of closed form formulas of the conditional and unconditional VG-CRBs. Indeed, in the near field case, the received power is variable from sensor to sensor which should be taken into account in the data model. By considering such variable gain model, we investigate the impact of the gain variation onto the localization performance limit.

Secondly, we consider a simple case where the sensor to sensor power variation is neglected[1] (i.e., Equal Gain

[1]To the best of our knowledge, this assumption is considered in all previous works.

(EG) model). The obtained EG-CRB expressions using the exact time delay values are then compared to those given in [15]. The development (i.e., Taylor expansion) of the exact EG-CRB allows us to highlight many interesting features including:

- A more accurate approximate EG-CRB for the exact model as compared to the EG-CRB based on an approximate model. In particular, we show that at low range values, the approximate EG-CRB in [15] can be up to 30 times larger than our exact EG-CRB.
- A detailed analysis of the source range parameter effect on its angle estimation performance[2].

Finally, we propose to exploit the exact CRB expression to specify the 'near field localization region' based on a desired localization performance. In that case, the 'near field localization region' is shown to depend not only on the source range parameter and array aperture but also on the sources SNR and observation sample size.

The paper is organized as follows: Section II introduces the data model and formulates the main paper objectives. In Section III, the conditional and unconditional VG-CRB derivations are provided in the variable gain case. Section IV presents the simple case where all sensors have the same gain (i.e., EG case). The EG-CRB is then compared to the VG-CRB with an analysis of the impact of the gain profile onto the localization performance. In addition, we show in section IV-B that considering the exact time delay expression leads to a more accurate CRB expression as compared to the CRB based on an approximate time delay. Section V introduces the concept of near field localization region and illustrates its usefulness through specific examples. Section VI is dedicated to simulation experiments while Section VII is for the concluding remarks.

II. Problem formulation

A. Data model

In this paper, we consider a uniform linear array with N sensors receiving a signal, emitted from one source located in the NF region, and corrupted by circular white Gaussian noise v_n of covariance matrix $\sigma^2\mathbf{I}_N$. The n^{th} array output, $n = 0, \cdots, N-1$, is expressed as

$$x_n(t) = \gamma_n(\theta, r)s(t)e^{j\tau_n(\theta,r)} + v_n(t) = s(t)(\gamma_n(\theta, r)e^{j\tau_n(\theta,r)}) + v_n(t) \quad t = 1, \cdots, T, \tag{1}$$

[2]Part of the work related to the EG-CRB has been published in [16] presented at conference ISSPA 2012.

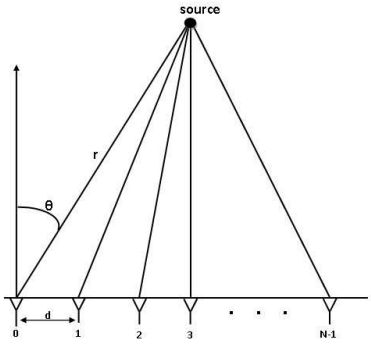

Fig. 1. Near field source model

where T is the sample size and $\gamma_n(\theta, r)$ represents the power profile of the n^{th} sensor given by [17]

$$\gamma_n(\theta, r) = \frac{1}{l_n} = \frac{1}{r\sqrt{1 - \frac{2nd}{r}\sin\theta + \left(\frac{nd}{r}\right)^2}}, \tag{2}$$

l_n being the distance between the source signal and the n^{th} sensor and $s(t)$ is the emitted signal. The exact expression of the time delay[3] τ_n is given by

$$\tau_n = \frac{2\pi r}{\lambda}\left(\sqrt{1 + \frac{n^2d^2}{r^2} - \frac{2nd\sin\theta}{r}} - 1\right), \tag{3}$$

where d is the inter-element spacing, λ is the propagation wavelength and (r, θ) are the polar coordinates of the source as shown in Fig. 1.

In the sequel, the source signal will be treated either as deterministic (conditional model) or stochastic (unconditional model). Indeed, in the array processing, both models can be found:

1) Conditional model in which the source signal is assumed deterministic but its parameters are unknown.
2) Unconditional model in which we assume that the source signal is random. In our case, we will assume $s(t)$ to be a complex circular Gaussian process with zero mean and unknown variance σ_s^2. Note that all existing works on the near field CRB consider such a Gaussian assumption. Indeed, in the Gaussian case, the CRB derivation is tractable and 'interpretable' closed form expressions can be obtained. In addition, as shown in [18] and [19], the Gaussian case is the least favorable one and hence it represents the most conservative choice. In other words, any optimization based on the CRB under the Gaussian assumption can be considered to be min-max optimal in the sense of minimizing the largest CRB.

[3]The first sensor, $n = 0$, is considered for the time reference.

Remark: Note that, the more general case of multipath channel is not considered here for the 'tractability' of the CRB derivation and its 'readability'. Indeed, in most existing papers, e.g. [12], one associates to each source one direction of arrival (i.e., one channel path). The source localization in multipath case can be treated as a multiple correlated sources case as in [20].

B. Objectives

In the literature, only approximate models of the received NF signals are considered. Indeed, two simplifications of the model in (1) are used in practice:

(a) The sensor to sensor power variation is neglected and the power profile is approximated by $\gamma_n(\theta, r) = \frac{1}{r}$. This model is referred to as the equal gain model since $\gamma_n(\theta, r)$ is constant with respect to the sensor index n.

(b) Also, most existing works on near field source localization consider the following approximation of the time delay expression to derive simple localization algorithms as well as CRB expressions, e.g., [21] [15]

$$\tau_n = -2\pi\frac{dn}{\lambda}\sin(\theta) + \pi\frac{d^2n^2}{\lambda}\frac{1}{r}\cos^2(\theta) + o\left(\frac{d}{r}\right). \tag{4}$$

The latter is considered as a good approximation of (3) in the Fresnel region given by [17]

$$0.62\left(\frac{d^3(N-1)^3}{\lambda}\right)^{\frac{1}{2}} < r < 2\frac{d^2(N-1)^2}{\lambda}. \tag{5}$$

Our first objective is to derive CRB expressions without these approximations, i.e.,

1) The distance from the source to the n^{th} sensor l_n is a function of the sensor position (i.e., sensor index) according to

$$l_n = \sqrt{r^2 - 2ndr\sin(\theta) + n^2d^2} = r\sqrt{1 - 2\frac{nd}{r}\sin(\theta) + \left(\frac{nd}{r}\right)^2}. \tag{6}$$

Hence, the received power profile is variable from sensor to sensor. In the far field case, this variation is negligible but not necessarily in the near field context. To the best of our knowledge, this point has not been taken into consideration in the existing literature. We would like to investigate the impact of such gain variation into the localization performance limit.

2) Based on the exact expression of the time delay τ_n in equation (3), we aim to derive the exact conditional and unconditional EG-CRB and show that the exact EG-CRB can be significantly different from the approximate EG-CRB given in [15].

Our second objective is to exploit the previous CRB derivation to better define the NF region according to a target localization performance, i.e.,

3) The near field region has been so far assimilated to the Fresnel region which depends on the antenna size and the signal wavelength only. However, the localization performance depends on other system parameters (SNR, sample size, angle position, $\cdots$) for which reason we introduce the concept of Near Field Localization Region (NFLR) where the localization error is upper bounded by a desired threshold value depending on the considered application. Based on the NFLR concept, we illustrate how the 'controllable' system parameters can be tuned to achieve a minimum target performance.

III. Conditional and unconditional CRB derivation with Variable Gain

In this case, we consider the model given by (1). As we can see, in this model both the time delay and the power profile carry information on the desired source location (θ, r). Our objective here, is to investigate the roles of both profiles in the performance limit given by the CRB.

A. Conditional VG-CRB

In this Section, we consider the source signal as deterministic according to the model

$$s(t) = \alpha(t)e^{j(2\pi f_0 t + \psi(t))},$$

where f_0 is the known carrier frequency while $\alpha(t)$ and $\psi(t)$ are the unknown amplitude and phase parameters of the source signal. Under the data model assumption of Section II-A, we derive next the exact deterministic (i.e., conditional) VG-CRB for the location parameter estimation.

1) Conditional VG-CRB derivation: The log-likelihood function of the observations is given by

$$L_c(\boldsymbol{\xi}^c) = -NT\ln\pi - NT\ln\sigma^2 - \frac{1}{\sigma^2}\left\|\boldsymbol{x} - \boldsymbol{\mu}\right\|^2, \tag{7}$$

where

$$\boldsymbol{x} = [\mathbf{x}^T(1)\cdots,\cdots,\mathbf{x}^T(T)]^T, \tag{8}$$

$$\mathbf{x}(t) = [x_0(t),\cdots,x_{N-1}(t)]^T, \tag{9}$$

$$\boldsymbol{\mu} = [s(1)\boldsymbol{a}^T(\theta,r),\cdots,s(T)\boldsymbol{a}^T(\theta,r)]^T, \tag{10}$$

$$\boldsymbol{a}(\theta,r) = [\gamma_0(\theta,r),\gamma_1 e^{j\tau_1(\theta,r)},\cdots,\gamma_{_{N-1}}(\theta,r)e^{j\tau_{N-1}(\theta,r)}]^T, \tag{11}$$

$$\boldsymbol{\xi}^c = [\theta,r,\boldsymbol{\Psi}^T,\boldsymbol{\alpha}^T,\sigma^2]^T, \tag{12}$$

$$\boldsymbol{\Psi} = [\psi(1),\cdots,\psi(T)]^T, \tag{13}$$

$$\boldsymbol{\alpha} = [\alpha(1),\cdots,\alpha(T)]^T, \tag{14}$$

$\|.\|$ refers to the Frobenius norm and $[.]^T$ is the transpose operator.

The CRB is equal to the inverse of the Fisher Information Matrix (FIM) defined by[4]

$$[\text{FIM}(\boldsymbol{\xi}^c)]_{i,j} = E\left(\frac{\partial L_c(\boldsymbol{\xi}^c)}{\partial\xi_i}\frac{\partial L_c(\boldsymbol{\xi}^c)}{\partial\xi_j}\right). \tag{15}$$

The latter is given in our particular case by

$$[\text{FIM}(\boldsymbol{\xi}^c)]_{i,j} = \frac{NT}{\sigma^4}\frac{\partial\sigma^2}{\partial\xi_i}\frac{\partial\sigma^2}{\partial\xi_j} + \frac{2}{\sigma^2}\Re\{\frac{\partial\boldsymbol{\mu}^H}{\partial\xi_i}\frac{\partial\boldsymbol{\mu}}{\partial\xi_j}\}, \tag{16}$$

where $\Re\{.\}$ refers to the real part of a complex valued entity. The FIM is given by the block diagonal matrix as

$$\text{FIM} = \begin{bmatrix} \boldsymbol{Q} & \mathbf{0}_{(2T+2)\times 1} \\ \mathbf{0}_{1\times(2T+2)} & \frac{NT}{\sigma^4} \end{bmatrix}, \tag{17}$$

where

$$\boldsymbol{Q} = \left[\begin{array}{cc|cc} f_{\theta\theta} & f_{\theta r} & \mathbf{f}_{\theta\psi} & \mathbf{f}_{\theta\alpha} \\ f_{r\theta} & f_{rr} & \mathbf{f}_{r\psi} & \mathbf{f}_{r\alpha} \\ \hline \mathbf{f}_{\psi\theta} & \mathbf{f}_{\psi r} & \mathbf{F}_{\psi\psi} & \mathbf{F}_{\psi\alpha} \\ \mathbf{f}_{\alpha\theta} & \mathbf{f}_{\alpha r} & \mathbf{F}_{\alpha\psi} & \mathbf{F}_{\alpha\alpha} \end{array}\right], \tag{18}$$

[4]All expected values are taken with respect to the distribution of the observation vector $\boldsymbol{x}$.

$$f_{\theta\theta} = 2TD_{\text{SNR}}(\|\dot{\boldsymbol{\gamma}}_\theta\|^2 + (\boldsymbol{\gamma}\odot\boldsymbol{\gamma})^T(\dot{\boldsymbol{\tau}}_\theta\odot\dot{\boldsymbol{\tau}}_\theta)), \tag{19}$$

$$f_{rr} = 2TD_{\text{SNR}}(\|\dot{\boldsymbol{\gamma}}_r\|^2 + (\boldsymbol{\gamma}\odot\boldsymbol{\gamma})^T(\dot{\boldsymbol{\tau}}_r\odot\dot{\boldsymbol{\tau}}_r)), \tag{20}$$

$$f_{r\theta} = f_{\theta r} = 2TD_{\text{SNR}}((\dot{\boldsymbol{\gamma}}_\theta^T\dot{\boldsymbol{\gamma}}_r) + (\boldsymbol{\gamma}\odot\boldsymbol{\gamma})^T(\dot{\boldsymbol{\tau}}_\theta\odot\dot{\boldsymbol{\tau}}_r)), \tag{21}$$

$$\boldsymbol{\gamma} = \left[\gamma_0(\theta,r),...,\gamma_{N-1}(\theta,r)\right]^T, \tag{22}$$

$$\dot{\boldsymbol{\gamma}}_\theta = \left[\frac{\partial\gamma_0}{\partial\theta},...,\frac{\partial\gamma_{N-1}}{\partial\theta}\right]^T, \tag{23}$$

$$\dot{\boldsymbol{\gamma}}_r = \left[\frac{\partial\gamma_0}{\partial r},...,\frac{\partial\gamma_{N-1}}{\partial r}\right]^T, \tag{24}$$

$$\boldsymbol{\tau} = \left[\tau_0(\theta,r),...,\tau_{N-1}(\theta,r)\right]^T, \tag{25}$$

$$\dot{\boldsymbol{\tau}}_\theta = \left[\frac{\partial\tau_0}{\partial\theta},...,\frac{\partial\tau_{N-1}}{\partial\theta}\right]^T, \tag{26}$$

$$\dot{\boldsymbol{\tau}}_r = \left[\frac{\partial\tau_0}{\partial r},...,\frac{\partial\tau_{N-1}}{\partial r}\right]^T, \tag{27}$$

and where $\odot$ represents the Hadamard product and $D_{\text{SNR}} = \frac{\|\boldsymbol{\alpha}\|^2}{T\sigma^2}$. Moreover, the vectors of size $T\times 1$, $\mathbf{f}_{\psi\theta}$, $\mathbf{f}_{\psi r}$, $\mathbf{f}_{\alpha\theta}$ and $\mathbf{f}_{\alpha r}$ are given by

$$\mathbf{f}_{\psi\theta} = \mathbf{f}_{\theta\psi}^T = \frac{2}{\sigma^2}(\boldsymbol{\gamma}\odot\boldsymbol{\gamma})^T\dot{\boldsymbol{\tau}}_\theta(\boldsymbol{\alpha}\odot\boldsymbol{\alpha}), \tag{28}$$

$$\mathbf{f}_{\psi r} = \mathbf{f}_{r\psi}^T = \frac{2}{\sigma^2}(\boldsymbol{\gamma}\odot\boldsymbol{\gamma})^T\dot{\boldsymbol{\tau}}_r(\boldsymbol{\alpha}\odot\boldsymbol{\alpha}), \tag{29}$$

$$\mathbf{f}_{\alpha\theta} = \mathbf{f}_{\theta\alpha}^T = \frac{2}{\sigma^2}(\boldsymbol{\gamma}^T\dot{\boldsymbol{\gamma}}_\theta)\boldsymbol{\alpha}, \tag{30}$$

$$\mathbf{f}_{\alpha r} = \mathbf{f}_{r\alpha}^T = \frac{2}{\sigma^2}(\boldsymbol{\gamma}^T\dot{\boldsymbol{\gamma}}_r)\boldsymbol{\alpha}. \tag{31}$$

Finally, matrices $\mathbf{F}_{\psi\psi}$, $\mathbf{F}_{\alpha\alpha}$, $\mathbf{F}_{\psi\alpha}$ of size $T\times T$, are given by

$$\mathbf{F}_{\psi\psi} = \frac{2}{\sigma^2}\|\boldsymbol{\gamma}\|^2\,\text{diag}(\boldsymbol{\alpha}\odot\boldsymbol{\alpha}), \quad \mathbf{F}_{\alpha\alpha} = \frac{2}{\sigma^2}\|\boldsymbol{\gamma}\|^2\,\mathbf{I}_T \quad \text{and} \quad \mathbf{F}_{\alpha\psi} = \mathbf{F}_{\psi\alpha} = \mathbf{0}_{T\times T}. \tag{32}$$

$\text{diag}(\boldsymbol{\alpha}\odot\boldsymbol{\alpha})$ refers to the diagonal matrix formed from vector $\boldsymbol{\alpha}\odot\boldsymbol{\alpha}$.

Equation (17) translates the fact that the FIM of the desired localization parameters is decoupled from the noise variance σ^2 but not from the source magnitude and phase parameters. Hence, the CRB matrix of the range and angle parameters is equal to the 2×2 top left sub-matrix of the inverse matrix $\boldsymbol{Q}^{-1}$. By using the Schur's matrix inversion lemma, one can obtain:

Lemma 1: The non-matrix expressions of the conditional CRB in the variable gain case for a source in the near field, for $N\geq 3$ and $\theta\neq\pm\frac{\pi}{2}$, are given by

$$\boxed{\begin{aligned}\text{VG-CRB}^c(\theta) &= \left(\tfrac{1}{2TD_{\text{SNR}}}\right)\tfrac{E_{vg}(r)}{E_{vg}(\theta)E_{vg}(r)-E_{vg}(\theta,r)^2}, \quad (33)\\ \text{VG-CRB}^c(r) &= \left(\tfrac{1}{2TD_{\text{SNR}}}\right)\tfrac{E_{vg}(\theta)}{E_{vg}(\theta)E_{vg}(r)-E_{vg}(\theta,r)^2}, \quad (34)\\ \text{VG-CRB}^c(\theta,r) &= \left(\tfrac{1}{2TD_{\text{SNR}}}\right)\tfrac{E_{vg}(\theta,r)}{E_{vg}(\theta)E_{vg}(r)-E_{vg}(\theta,r)^2}, \quad (35)\end{aligned}}$$

where

$$E_{vg}(\theta) = \|\dot{\boldsymbol{\gamma}}_\theta\|^2 + (\boldsymbol{\gamma}\odot\boldsymbol{\gamma})^T(\dot{\boldsymbol{\tau}}_\theta\odot\dot{\boldsymbol{\tau}}_\theta) - \frac{1}{\|\boldsymbol{\gamma}\|^2}\left[((\boldsymbol{\gamma}\odot\boldsymbol{\gamma})^T\dot{\boldsymbol{\tau}}_\theta)^2 + (\boldsymbol{\gamma}^T\dot{\boldsymbol{\gamma}}_\theta)^2\right], \quad (36)$$

$$E_{vg}(r) = \|\dot{\boldsymbol{\gamma}}_r\|^2 + (\boldsymbol{\gamma}\odot\boldsymbol{\gamma})^T(\dot{\boldsymbol{\tau}}_r\odot\dot{\boldsymbol{\tau}}_r) - \frac{1}{\|\boldsymbol{\gamma}\|^2}\left[((\boldsymbol{\gamma}\odot\boldsymbol{\gamma})^T\dot{\boldsymbol{\tau}}_r)^2 + (\boldsymbol{\gamma}^T\dot{\boldsymbol{\gamma}}_r)^2\right], \quad (37)$$

$$E_{vg}(\theta,r) = \dot{\boldsymbol{\gamma}}_\theta^T\dot{\boldsymbol{\gamma}}_r + (\boldsymbol{\gamma}\odot\boldsymbol{\gamma})^T(\dot{\boldsymbol{\tau}}_\theta\odot\dot{\boldsymbol{\tau}}_r) - \frac{1}{\|\boldsymbol{\gamma}\|^2}\left[(\boldsymbol{\gamma}\odot\boldsymbol{\gamma})^T\dot{\boldsymbol{\tau}}_\theta(\boldsymbol{\gamma}\odot\boldsymbol{\gamma})^T\dot{\boldsymbol{\tau}}_r + (\boldsymbol{\gamma}^T\dot{\boldsymbol{\gamma}}_r)(\boldsymbol{\gamma}^T\dot{\boldsymbol{\gamma}}_\theta)\right]. \quad (38)$$

Proof: See appendix A

B. Unconditional VG-CRB

For unconditional CRB, the signal is assumed Gaussian complex circular with zero mean and variance σ_s^2. In this case, the vector of the unknown parameters becomes $\boldsymbol{\xi}^u = [\theta, r, \sigma_s^2, \sigma^2]^T$, and then the log-likelihood function of the observed data is given by

$$L_u(\boldsymbol{\xi}^u) = -NT\ln\pi - \ln\det(\boldsymbol{\Sigma}) - T\text{tr}(\boldsymbol{\Sigma}^{-1}\hat{\mathbf{R}}), \quad (39)$$

where $\boldsymbol{\Sigma} = \sigma_s^2\boldsymbol{a}(\theta,r)\boldsymbol{a}(\theta,r)^H + \sigma^2\mathbf{I}_N$ (theoretical covariance matrix), $\hat{\mathbf{R}} = \frac{1}{T}\sum_{t=1}^{T}\boldsymbol{x}(t)\boldsymbol{x}^H(t)$ (sample estimate covariance matrix), tr(.) (respectively det(.)) refers to the matrix trace (respectively matrix determinant) and $(.)^H$ is the transpose conjugate operator.

Under the assumption of the Gaussian stochastic signals, the $(i,j), 1\leq i,j\leq 4$ entries of the FIM are given by

$$[\text{FIM}(\boldsymbol{\xi}^u)]_{i,j} = T\text{tr}\left(\boldsymbol{\Sigma}^{-1}\frac{\partial\boldsymbol{\Sigma}}{\partial\xi_i}\boldsymbol{\Sigma}^{-1}\frac{\partial\boldsymbol{\Sigma}}{\partial\xi_j}\right). \quad (40)$$

Since the CRB is equal to the inverse of the Fisher information matrix and using the results of [22] for the two desired localization parameters, we have the following lemma:

Lemma 2: The non-matrix expressions of the exact unconditional CRB in the variable case for a source in the near field, for $N\geq 3$ and $\theta\neq\pm\frac{\pi}{2}$, are given by

$$\text{VG-CRB}^{u}(\theta) = \left[\frac{(1+\text{SNR}\|\boldsymbol{\gamma}\|^2)D_{\text{SNR}}}{(\text{SNR})^2\|\boldsymbol{\gamma}\|^2}\right]\text{VG-CRB}^{c}(\theta), \quad (41)$$

$$\text{VG-CRB}^{u}(r) = \left[\frac{(1+\text{SNR}\|\boldsymbol{\gamma}\|^2)D_{\text{SNR}}}{(\text{SNR})^2\|\boldsymbol{\gamma}\|^2}\right]\text{VG-CRB}^{c}(r), \quad (42)$$

$$\text{VG-CRB}^{u}(\theta,r) = \left[\frac{(1+\text{SNR}\|\boldsymbol{\gamma}\|^2)D_{\text{SNR}}}{(\text{SNR})^2\|\boldsymbol{\gamma}\|^2}\right]\text{VG-CRB}^{c}(\theta,r), \quad (43)$$

where $\text{SNR} = \frac{\sigma_s^2}{\sigma^2}$.

Proof: See appendix B

IV. Conditional and unconditional CRB derivation with Equal Gain

Here, we consider the particular case of equal gain usually considered in the literature. Our objective is twofold: (i) the derived EG-CRB expressions are compared with the EG-CRB of the approximate model given by El Korso in [15] in order to highlight the impact of the time delay approximation on the CRB, (ii) then comparisons between equal gain and variable gain cases are made, by deriving the Taylor expansion of the proposed expressions of the CRB, in order to exhibit the impact of the variation of the power profile on the estimation performance.

A. Conditional and unconditional EG-CRB derivation

For the equal gain case, we do not consider the variation of the power profile which is equivalent to assuming that all sensors have equal gain (i.e., $\gamma_n(\theta,r) \approx \frac{1}{r} \ \ \forall n$). In that case, since the transmit source power is unknown, the factor $\frac{1}{r}$ is incorporated into the source amplitude that are redefined according to

$$\tilde{\boldsymbol{\alpha}} = \frac{1}{r}\boldsymbol{\alpha} \quad \text{in the deterministic case} \quad (44)$$

or

$$\tilde{\sigma}_s = \frac{1}{r}\sigma_s \quad \text{in the stochastic case} \quad (45)$$

1) Conditional EG-CRB: Here, the received signal at the n^{th} sensor is given by

$$x_n(t) = s(t)e^{\jmath\tau_n} + v_n(t), \quad (46)$$

with $s(t) = \tilde{\alpha}(t)e^{\jmath(\psi(t)+f_0 t)}$. The corresponding CRB expressions can be deduced from the one in lemma 1 by replacing $\boldsymbol{\alpha}$ by $\tilde{\boldsymbol{\alpha}}$ and setting $\boldsymbol{\gamma} = \mathbf{1}_N$ and $\dot{\boldsymbol{\gamma}}_\theta = \dot{\boldsymbol{\gamma}}_r = \mathbf{0}$ where all entries of the vector $\mathbf{1}_N$ of size $(N \times 1)$ are equal to 1. We obtain then the following results:

Lemma 3: The non-matrix expressions of the conditional CRB in the equal gain case for a source in the near field, for $N \geq 3$ and $\theta \neq \pm\frac{\pi}{2}$, are given by

$$\boxed{\begin{aligned}\text{EG-CRB}^c(\theta) &= \left(\tfrac{1}{2T\tilde{D}_{\text{SNR}}}\right)\tfrac{E_{eg}(r)}{E_{eg}(\theta)E_{eg}(r)-E_{eg}(\theta,r)^2}, \quad (47)\\ \text{EG-CRB}^c(r) &= \left(\tfrac{1}{2T\tilde{D}_{\text{SNR}}}\right)\tfrac{E_{eg}(\theta)}{E_{eg}(\theta)E_{eg}(r)-E_{eg}(\theta,r)^2}, \quad (48)\\ \text{EG-CRB}^c(\theta,r) &= \left(\tfrac{1}{2T\tilde{D}_{\text{SNR}}}\right)\tfrac{E_{eg}(\theta,r)}{E_{eg}(\theta)E_{eg}(r)-E_{eg}(\theta,r)^2}, \quad (49)\end{aligned}}$$

where $\text{EG-CRB}^c(\theta,r)$ is the non diagonal entry of the considered 2×2 CRB matrix (it represents the coupling between the 2 parameters), $\tilde{D}_{\text{SNR}} = \frac{\|\tilde{\boldsymbol{\alpha}}\|^2}{T\sigma^2}$ and

$$\begin{aligned}E_{eg}(\theta) &= \|\dot{\boldsymbol{\tau}}_\theta\|^2 - \frac{1}{N}(\mathbf{1}_N^T\dot{\boldsymbol{\tau}}_\theta)^2, &(50)\\ E_{eg}(r) &= \|\dot{\boldsymbol{\tau}}_r\|^2 - \frac{1}{N}(\mathbf{1}_N^T\dot{\boldsymbol{\tau}}_r)^2, &(51)\\ E_{eg}(\theta,r) &= \dot{\boldsymbol{\tau}}_\theta^H\dot{\boldsymbol{\tau}}_r - \frac{1}{N}(\mathbf{1}_N^T\dot{\boldsymbol{\tau}}_\theta)(\mathbf{1}_N^T\dot{\boldsymbol{\tau}}_r). &(52)\end{aligned}$$

2) Taylor Expansion (TE) of conditional EG-CRB: This section aims to highlight the effects of some system parameters on the localization performance and to better compare, in section IV-B, our exact CRB with the CRB given in [15]. For that, we propose to use a Taylor expansion of the expressions of lemma 3. For simplicity, we omit the details of the cumbersome (but straightforward) derivations and present only the final results in the following lemma:

Lemma 4: The Taylor expansions of the exact CRB expressions of lemma 3 lead to

$$\begin{aligned}\text{EG-CRB}^c(\theta) &\approx \frac{3\lambda^2}{2T\tilde{D}_{\text{SNR}}d^2\pi^2\cos^2(\theta)p_3(N)}\times\Bigg[p_2(N)-6(N-1)(6N^2-15N+11)\sin(\theta)\frac{d}{r}\\ &\quad+\left\{\frac{1}{70}(2N-1)(384N^3-1353N^2+1379N-368)\right.\\ &\quad\left.+\frac{1}{14}(186N^4-1590N^3+5351N^2-6795N+2890)\sin^2(\theta)\right\}\frac{d^2}{r^2}\Bigg], &(53)\\ \text{EG-CRB}^c(r) &\approx \frac{6r^2\lambda^2}{T\tilde{D}_{\text{SNR}}d^4\pi^2\cos^4(\theta)p_3(N)}\times\Big[15r^2-60(N-1)\sin(\theta)dr\\ &\quad+\frac{1}{14}\left\{\sin^2(\theta)(1061N^2-2625N+2911)+225N^2-315N-135\right\}d^2\Bigg], &(54)\end{aligned}$$

where $p_2(N) = (8N-11)(2N-1)$ and $p_3(N) = N(N^2-1)(N^2-4)$.

These expressions are useful to compare our CRB to the one in [15] but also, they allow us to better reveal how the different system parameters affect the localization performance. For example, one can see in particular that:

- The CRB decreases linearly with respect to the observation time as well as the deterministic SNR, i.e., $\tilde{D}_{\text{SNR}}$
- The CRB goes to infinity when $\theta \to \pm\frac{\pi}{2}$ and the best localization results are obtained in the central direction, i.e., for $\theta = 0$.
- Asymptotically (for large antenna sizes), the first term of the TE in (53) decreases in N^3, i.e., if we double the number of sensors, the CRB will be decreased approximately by a factor of 8.

3) Unconditional EG-CRB: The EG-CRB in that case can be obtained from the VG-CRB by setting $\boldsymbol{\gamma} = \mathbf{1}_N$ and $\tilde{\sigma}_s^2 = \frac{\sigma_s^2}{r^2}$:

Lemma 5: The non-matrix expressions of the unconditional CRB in the equal gain case for a source in the near field, for $N \geq 3$ and $\theta \neq \pm\frac{\pi}{2}$ are given by

$$\text{EG-CRB}^u(\theta) = \left[\frac{(1+(\tilde{\text{SNR}})\quad N)\tilde{D}_{\text{SNR}}}{(\tilde{\text{SNR}})^2\quad N}\right]\text{EG-CRB}^c(\theta), \tag{55}$$

$$\text{EG-CRB}^u(r) = \left[\frac{(1+(\tilde{\text{SNR}})\quad N)\tilde{D}_{\text{SNR}}}{(\tilde{\text{SNR}})^2\quad N}\right]\text{EG-CRB}^c(r), \tag{56}$$

$$\text{EG-CRB}^u(\theta, r) = \left[\frac{(1+(\tilde{\text{SNR}})\quad N)\tilde{D}_{\text{SNR}}}{(\tilde{\text{SNR}})^2\quad N}\right]\text{EG-CRB}^c(\theta, r), \tag{57}$$

where $\tilde{\text{SNR}} = \frac{\tilde{\sigma}_s^2}{\sigma^2}$ and $\tilde{D}_{\text{SNR}} \times \text{EG-CRB}^c$ represents the normalized EG-CRB^c (see lemma 3) depending on the localization parameters, the array geometry, and the sample size only.

This result translates the fact that the unconditional CRB varies in a similar way as the conditional CRB with respect to variables θ, r and T. However, concerning the SNR parameter and the number of sensors, it is interesting to observe that:

- At low SNRs (i.e., if $\tilde{\text{SNR}} \times N << 1$), the CRB decreases quadratically (instead of linearly in the conditional case) with respect to the SNR and in N^4 (instead of N^3) in terms of the number of sensors.
- However, for large SNRs (i.e., if $\tilde{\text{SNR}} \times N >> 1$), the unconditional CRB behaves similarly to the conditional CRB with respect to parameters $\tilde{\text{SNR}}$ and N (i.e., it decreases linearly with $\tilde{\text{SNR}}$ and in N^3 with respect to the number of sensors).

B. Comparison with the 'EG-CRB of the approximate model'

Let us first recall the CRB expressions[5] given in [15] and based on the approximate model in (4) referred to as EG-CRB^a where the subscript 'a' stands for 'approximate':

Lemma 6: The non-matrix expressions of the approximate conditional CRB [15] for a source in the near field, for $N \geq 3$ and $\theta \neq \pm\frac{\pi}{2}$, are given by

$$\text{EG-CRB}^a(\theta) = \frac{3\lambda^2}{2T\tilde{D}_{\text{SNR}}d^2\pi^2\cos^2(\theta)p_3(N)}p_2(N), \tag{58}$$

$$\text{EG-CRB}^a(r) = \frac{6r^2\lambda^2}{T\tilde{D}_{\text{SNR}}d^4\pi^2\cos^4(\theta)p_3(N)}\left(15r^2 + 30dr(N-1)\sin(\theta) + d^2p_2(N)\sin^2(\theta)\right). \tag{59}$$

Comparing lemma 4 to lemma 6, one can make the following observations:

- First, we note that the first and main term of equation (53) (respectively of equation (54)) is equal to the first term of equation (58) (respectively of equation (59)).
- We note also, that the Taylor expansion (of the time delay) followed by CRB derivation leads to different results as compared to CRB derivation followed by Taylor expansion (of the CRB). The latter expansion being more accurate than the former as illustrated by our simulation results.
- The approximate CRB of the angle estimate shown in lemma 6 is independent of the range parameter (it is the same as the far field CRB) while the expression of EG-CRB$^c(\theta)$ in lemma 4 reveals how it is affected by the range parameter. In particular, at the first order, one can see that the CRB decreases (respectively increases) as a function of $\frac{d}{r}$ for $\theta \in [0, \frac{\pi}{2}[$ (respectively for $\theta \in]-\frac{\pi}{2}, 0]$).

C. Comparison between VG and EG cases

By considering the extra-information given by the received power profile, one is able to achieve in general better localization performance as will be shown later in Section VI. To better compare the CRB expressions in the

[5]We provide here the CRB for the conditional model only since it is equal to the CRB of the unconditional model up to a scalar constant (see lemma 2).

constant and variable gain cases, we provide here the dominant term of their Taylor expansion

$$\text{EG-CRB}^c(\theta) \approx \frac{3\lambda^2 p_2(N)}{2\pi^2 T\tilde{D}_{\text{SNR}} d^2\cos^2(\theta)p_3(N)}, \tag{60}$$

$$\text{VG-CRB}^c(\theta) \approx \frac{3\lambda^2 r^2 p_2(N)\left(1+\lambda^2 f_1(\theta)\right)}{2\pi^2 T D_{\text{SNR}} d^2\cos^2(\theta)p_3(N)\left(1+\lambda^2 f_2(\theta)\right)}, \tag{61}$$

$$\text{EG-CRB}^c(r) \approx \frac{90\lambda^2 r^4}{\pi^2 T\tilde{D}_{\text{SNR}} d^4\cos^4(\theta)p_3(N)}, \tag{62}$$

$$\text{VG-CRB}^c(r) \approx \frac{90\lambda^2 r^6}{\pi^2 T D_{\text{SNR}} d^4\cos^4(\theta)p_3(N)\left(1+\lambda^2 f_2(\theta)\right)}, \tag{63}$$

where $f_1(\theta) = \frac{15\sin^2(\theta)}{\pi^2 d^2\cos^4(\theta)p_2(N)}$ and $f_2(\theta) = \frac{15\sin^2(\theta)}{\pi^2 d^2\cos^4(\theta)(N^2-4)}$. Note that the dominant term of EG-CRB^c is larger than the dominant term of EV-CRB^c for both range and angle parameters.

From these expressions, one can see that the two CRBs are quite similar[6] for sources located in the central direction (i.e., for small θ values) while at lateral directions (i.e., $|\theta|$ close to $\frac{\pi}{2}$) the variable gain CRB is much lower than the equal gain one. This translates the fact that when the source location information contained in the time delay profile becomes weak, it is somehow partially compensated by the location information contained in the received power profile especially for the estimation of the range value. This observation is illustrated by the simulation experiments (cf. Fig. 4, Fig. 5 and Fig. 6) given in Section VI.

V. Near field localization region (NFLR)

The radiating near field or Fresnel region is the region between the near and far fields [17] corresponding to the space region defined by equation (5). The latter depends on the source-antenna range, the signal wavelength, and the antenna aperture.

Note that the lower bound of Fresnel region is related to the fact that in the immediate vicinity of the antenna, the fields are predominately reactive fields meaning that the E and H fields are orthogonal [17]. Therefore the space region given by $r \leq 0.62\left(\frac{d^3(N-1)^3}{\lambda}\right)^{\frac{1}{2}}$ should be kept out of the localization region. However, the upper bound of the Fresnel region as given in equation (5) does not take into consideration the localization performance limit. For this reason, we suggest to define the near field localization region (NFLR) based on a target estimation performance relative to the application at hand. More precisely, if $\text{Std}_{max} > 0$ is the maximum standard deviation

[6]Note that, due to the source amplitude normalization introduced in section IV-A, one has $\tilde{D}_{\text{SNR}} = \frac{D_{\text{SNR}}}{r^2}$.

of the localization error that is tolerated by the considered application[7], i.e.,

$$\sqrt{E\left(\|\hat{\mathbf{p}}-\mathbf{p}\|^2\right)} \leq \text{Std}_{max}, \tag{64}$$

where $\mathbf{p}=(x,y)^T$ (respectively $\hat{\mathbf{p}}$) refers to the position vector (respectively its estimate), then the NFL region can be defined as the one for which the minimum standard deviation (given by the square root of the CRB) satisfies condition (64).

Since $E\left(\|\hat{\mathbf{p}}-\mathbf{p}\|^2\right)=E((\hat{x}-x)^2)+E((\hat{y}-y)^2)$, the previous condition on the minimum MSE can be expressed as

$$\sqrt{\text{CRB}(x)+\text{CRB}(y)} \leq \text{Std}_{max}. \tag{65}$$

Now, the source coordinates can be rewritten according to

$$\begin{aligned} x &= r\sin(\theta)=g_x(\theta,r), \\ y &= r\cos(\theta)=g_y(\theta,r), \end{aligned}$$

and hence, by using the delta method in [25], one can express

$$\text{CRB}(x)+\text{CRB}(y)=\nabla g_x^T(\theta,r)\mathbf{C}\nabla g_x(\theta,r)+\nabla g_y^T(\theta,r)\mathbf{C}\nabla g_y(\theta,r), \tag{66}$$

where

$$\nabla g_x(\theta,r) = \left[\frac{\partial g_x}{\partial\theta} \quad \frac{\partial g_x}{\partial r}\right]^T = \left[r\cos(\theta) \quad \sin(\theta)\right]^T, \tag{67}$$

$$\nabla g_y(\theta,r) = \left[\frac{\partial g_y}{\partial\theta} \quad \frac{\partial g_y}{\partial r}\right]^T = \left[-r\sin(\theta) \quad \cos(\theta)\right]^T, \tag{68}$$

$$\mathbf{C} = \begin{bmatrix} \text{CRB}(\theta) & \text{CRB}(\theta,r) \\ \text{CRB}(\theta,r) & \text{CRB}(r) \end{bmatrix}. \tag{69}$$

A straightforward derivation of (66) leads to

$$\text{CRB}(x)+\text{CRB}(y)=r^2\text{CRB}(\theta)+\text{CRB}(r), \tag{70}$$

[7]For example, in mobile localization, it is required that in case of emergency the location error is less than 125 m [23] with a given confidence level. Also, for safety raisons, automatic vehicle navigation based on GPS or inertial measurement units, requires a maximal location error known as the 'safety location radius' [24].

and therefore the NFL region is defined as the one corresponding to

$$\sqrt{r^2\text{CRB}(\theta) + \text{CRB}(r)} \leq \text{Std}_{max}. \tag{71}$$

An alternative approach would be to use a maximum tolerance value on the relative location error, i.e., a given threshold value ϵ such that

$$\sqrt{\frac{E\left(\|\hat{\mathbf{p}} - \mathbf{p}\|^2\right)}{\|\mathbf{p}\|^2}} \leq \epsilon, \tag{72}$$

which corresponds to

$$\sqrt{\text{CRB}(\theta) + \frac{\text{CRB}(r)}{r^2}} \leq \epsilon. \tag{73}$$

For example, in the conditional case, equation (73) becomes

$$\frac{1}{2TD_{\text{SNR}}}\mathbf{G}_N(\theta, r) \leq \epsilon^2, \tag{74}$$

where

$$\mathbf{G}_N(\theta, r) = \frac{E_{vg}(\theta) + E_{vg}(r)/r^2}{E_{vg}(\theta)E_{vg}(r) - E_{vg}(\theta, r)^2}.$$

From a practical point of view, equation (74) can be used to tune the system parameters in order to achieve a desired localization performance. Different scenarios can be considered, according to the parameter, we can (or wish to) tune.

Scenario 1: One can define the minimum observation time to achieve a desired localization performance at a given location and a given SNR value as

$$T_{min}(\theta, r) = \frac{\mathbf{G}_N(\theta, r)}{2\epsilon^2 D_{\text{SNR}}}. \tag{75}$$

Similarly, one can also define the minimum SNR value for a target localization quality as

$$D_{\text{SNR}_{min}}(\theta, r) = \frac{\mathbf{G}_N(\theta, r)}{2\epsilon^2 T}. \tag{76}$$

In Section VI, we provide simulation examples to illustrate the variation of these two parameters with respect to the source location.

Scenario 2: The previous parameters can be also defined for a desired localization region R_d (instead of a single location point (θ, r)) as

$$T_{min}(R_d) = \max_{(\theta,r)\in R_d} T_{min}(\theta, r), \tag{77}$$

$$D_{\text{SNR}_{min}}(R_d) = \max_{(\theta,r)\in R_d} D_{\text{SNR}_{min}}(\theta, r). \tag{78}$$

For example, if we are interested into the surveillance of a space sector limited by $r_{min} < r < r_{max}$ and $-\theta_{max} < \theta < \theta_{max}$, then

$$T_{min} = \tfrac{1}{2\epsilon^2 D_{\text{SNR}}} \max_{R_d} \mathbf{G}_N(\theta, r) \approx \frac{1}{2\epsilon^2 D_{\text{SNR}}} \mathbf{G}_N(r_{max}, \theta_{max}), \tag{79}$$

$$D_{\text{SNR}_{min}} = \tfrac{1}{2\epsilon^2 T} \max_{R_d} \mathbf{G}_N(\theta, r) \approx \frac{1}{2\epsilon^2 T} \mathbf{G}_N(r_{max}, \theta_{max}), \tag{80}$$

where the second equality holds from the observation that, away from the origin, $\mathbf{G}_N$ is a decreasing function with respect to the angular and range parameters[8].

Scenario 3: One can also wish to optimize the number of sensors with respect to a desired localization region R_d and for a target localization quality ϵ. In that case, the minimum number of sensors needed to achieve the target quality can be calculated as

$$N_{min} = \arg\min_{N} \left\{ N \in \mathbb{N}^* \,\middle|\, \mathbf{G}_N(\theta, r) \leq 2\epsilon^2 T D_{\text{SNR}} \quad \forall (\theta, r) \in R_d \right\}. \tag{81}$$

VI. Simulation Results

In this section, three experimental sets are considered. The first one is to compare the provided exact EG-CRB expressions of lemma 3 with the CRB expressions given in [15]. In the second experiment, we investigate the effect of considering the variable gain model instead of the constant gain model for near field source localization. Finally, the third experiment is to illustrate the usefulness of the near field localization region as compared to the standard Fresnel region.

In all our simulations, we consider a uniform linear antenna with $N = 15$ sensors and inter-element spacing $d = \frac{\lambda}{2}$ ($\lambda = 0.5m$) receiving signals from one near field source located at (θ, r). The sample size is $T = 90$ (unless

[8]This is not an exact and proven statement but just an approximation that expresses the fact that the localization accuracy decreases when the source moves away from the antenna or towards its lateral directions.

stated otherwise) and the observed signal is corrupted by a white Gaussian circular noise of variance σ^2. In the conditional case, the source signal is of unit amplitude (i.e., $\tilde{\alpha}(t) = 1 \ \ \forall t$). The dotted vertical plots in all figures represent the upper and lower range limits of the Fresnel region given by (5).

A. Experiment 1: Comparison with existing work in the EG case

In Fig. 2, we compare the three EG-CRB expressions for the source location parameter estimates versus the range values in the interval $[0 \ , \ 50m]$ and versus angle values[9] in the interval $[-87^o \ , \ 87^o]$. The noise level is set to $\sigma^2 = 0.001$ (high SNR case). A similar comparison leading to similar results is given in Fig. 3 for a noise level set to $\sigma^2 = 0.5$ (low SNR case). The source angle is $\theta = 45^o$ in the comparison versus range values and $r = 20\lambda$ in the comparison versus angle values.

From these figures, one can make the following observations:

1) There is a non negligible difference between the exact EG-CRB and the proposed one in [15] especially at low range values: i.e., the given EG-CRB in [15] can be up to 30 times larger than the exact CRB.
2) From Fig. 2.(c) and Fig. 3.(c), contrary to the given CRB in [15], the exact one varies with the range value with a relative difference varying from approximately 60% for small ranges to 0 when r goes to infinity.
3) From Fig. 2.(b) - Fig. 3.(b), one can observe that the lowest CRB is obtained in the central directions. This observation can be seen from the TE given in lemma 4 where the factor $\frac{1}{\cos(\theta)}$ is minimum for this directions and goes to infinity[10] when $|\theta| \rightarrow \frac{\pi}{2}$.
4) We note that the provided Taylor expansion of the exact CRB is more accurate than the one obtained by expanding the time delay expression before CRB derivation i.e., the one in [15].

B. Experiment 2: EG versus VG cases

To this end, we have to ensure first that the received power in the two cases (i.e., constant and variable gain cases) is the same for the reference sensor (i.e., dividing the power of constant gain case per the square of the range

[9]Note that the curves with respect to the angle parameter (i.e., Fig. 2, Fig. 3, Fig. 6, Fig. 9 and Fig. 10) are not symmetrical around $\theta = 0$ because we have chosen the first sensor for the time reference as shown in Fig. 1.

[10]This is due to the fact that the angle parameter is not observed directly but only through the $\sin$ function, which translates the fact that 'weak information' is carried by the observed data on the source location parameters in the lateral directions.

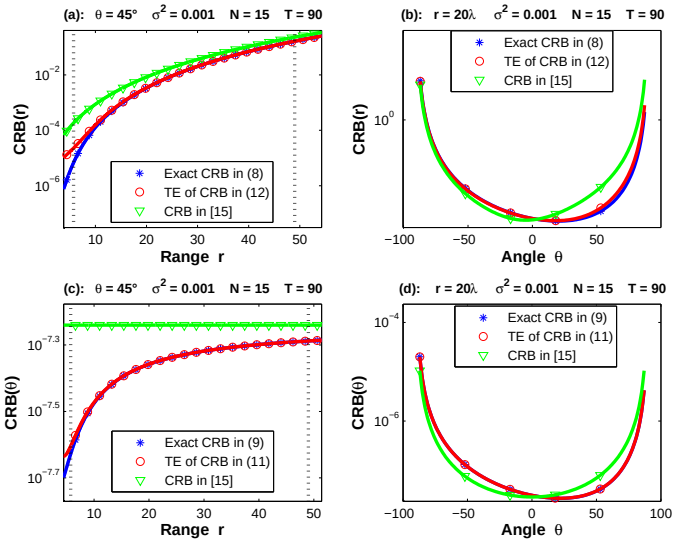

Fig. 2. CRB comparison: Exact conditional CRB versus approximate CRB in [15] in low SNR case

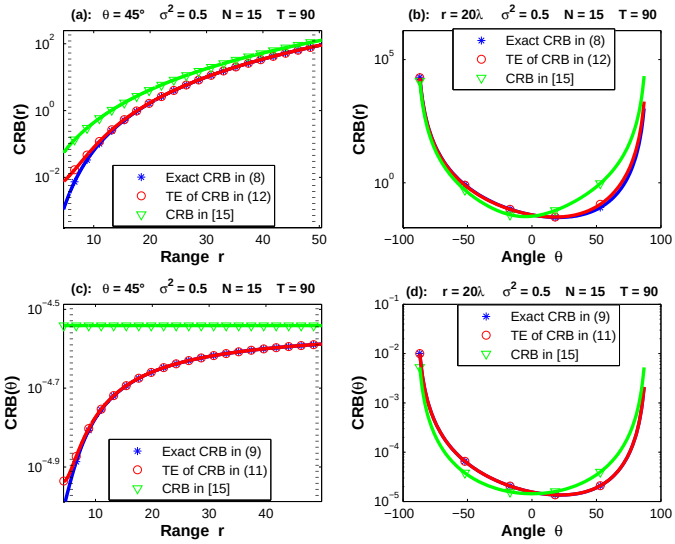

Fig. 3. CRB comparison: Exact conditional CRB versus approximate CRB in [15] in low SNR case

as explained in section IV-A). To better compare the CRB expressions, we consider two contexts where $\theta = 0^o$ for the first one (central direction) and $\theta = 85^o$ for the second one (lateral direction). One can observe from Fig. 4 and Fig. 5 that, for small $|\theta|$ values, the constant gain CRB is quite similar to the variable gain one while at lateral direction (i.e., $|\theta|$ close to $\frac{\pi}{2}$) the variable gain CRB is much lower than the equal gain one, due to the extra information brought by the considered gain profile.

This can be seen again from Fig. 6 where we can observe the large CRB difference for high $|\theta|$ values. In brief, one can say that when the 'location information' contained in the time delay is relatively weak (which is the

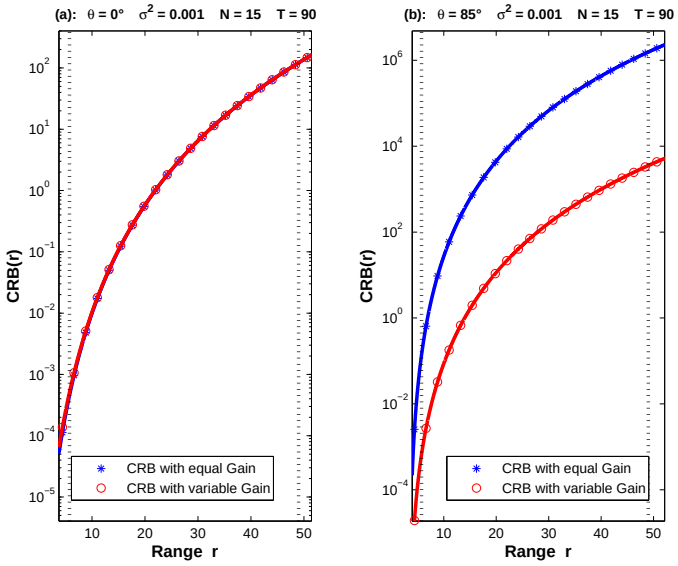

Fig. 4. CRB comparison: Equal Gain versus Variable Gain cases for range estimation

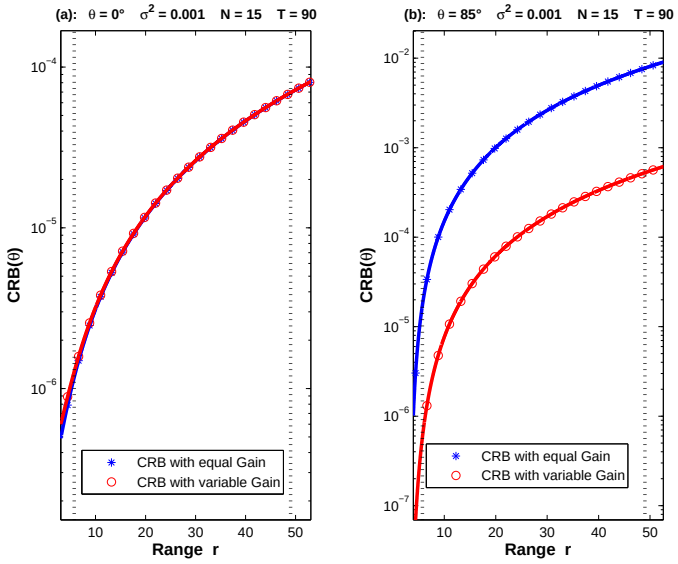

Fig. 5. CRB comparison: Equal Gain versus Variable Gain cases for angle estimation

case for sources located in the lateral directions) the information obtained by considering the power profile would significantly help improving the source location estimation.

C. Experiment 3: Near Field Localization Region

The plots in Fig. 7 represent the upper limit of the NFL region for different tolerance values. From this figure, one can observe that the Fresnel region is not appropriate to characterize the localization performance. Indeed, depending on the target quality, one can have space locations (i.e., sub-regions) in the Fresnel region that are out

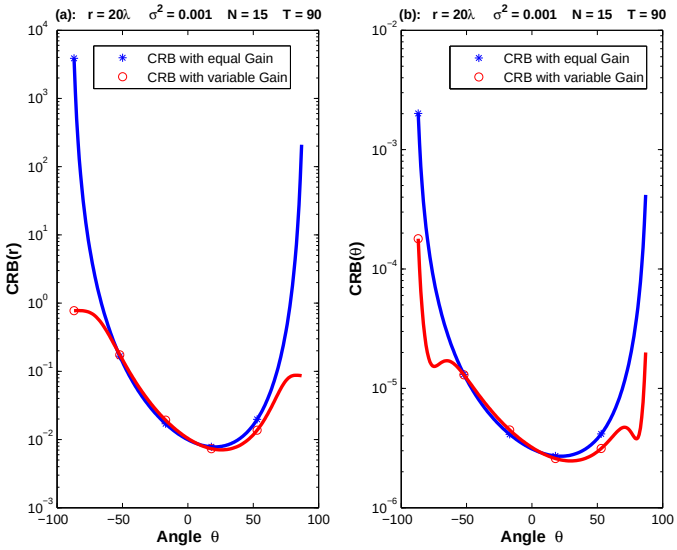

Fig. 6. CRB comparison of the Equal Gain and Variable Gain cases versus angle value

of the NFLR. Inversely, we have space locations not part of the Fresnel region that are attainable, i.e., they belong to the NFLR.

Fig. 8 compares the NFL region in the variable gain and equal gain cases with $D_{\text{SNR}} = 30\ dB$. One can observe that in the lateral directions the NFLR associated to the variable gain model is much larger than its counterpart associated to the equal gain one. Also, in the short observation time context (i.e., Fig. 8.(a)) the NFLR is included in the Fresnel region while for large observation time (i.e., Fig. 8.(b)) the NFLR region is much more expanded and contains most of the Fresnel region[11].

In Fig. 9 - Fig. 10, we illustrate the variation of the two parameters T_{min} and $D_{\text{SNR}_{min}}$ with respect to the source location parameters and for a relative tolerance error equal to $\epsilon = 10\%$. From these figures, one can observe that $D_{\text{SNR}_{min}}$ and T_{min} increase significantly for sources that are located far from the antenna or in the lateral directions.

VII. Conclusion

In this paper, three important results are proposed, discussed, and assessed through theoretical derivations and simulation experiments: (i) Exact EG conditional and unconditional CRB derivation for near field source localization and its development in non matrix form. The latter reveals interesting features and interpretations not shown by the CRB given in the literature based on an approximate model (i.e., approximate time delay). (ii) CRB derivation for

[11]Except for the extreme lateral directions where the target quality can never be met since the CRB goes to infinity for $|\theta| \to \frac{\pi}{2}$.

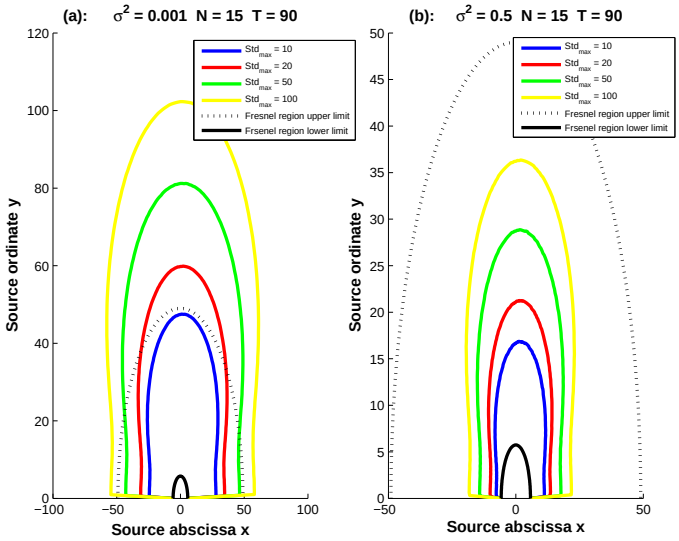

Fig. 7. Near field localization regions for different values of the target quality: Std_{max}

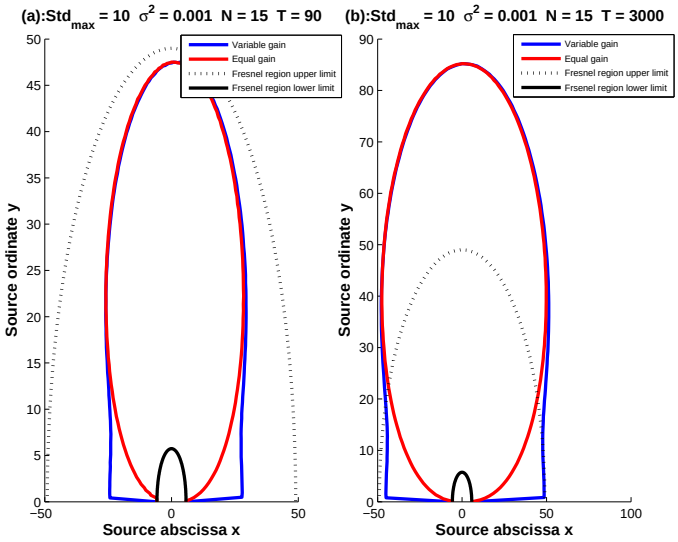

Fig. 8. Comparison of NFL regions in equal and variable gain cases

the VG case which investigates the importance of the power profile information in 'adverse' localization contexts and particularly for lateral lookup directions. (iii) Based on the previous CRB derivations, a new concept of 'localization region' is introduced to better define the space region where the localization quality can meet a target value or otherwise to better tune the system parameters to achieve the target localization quality for a given location region.

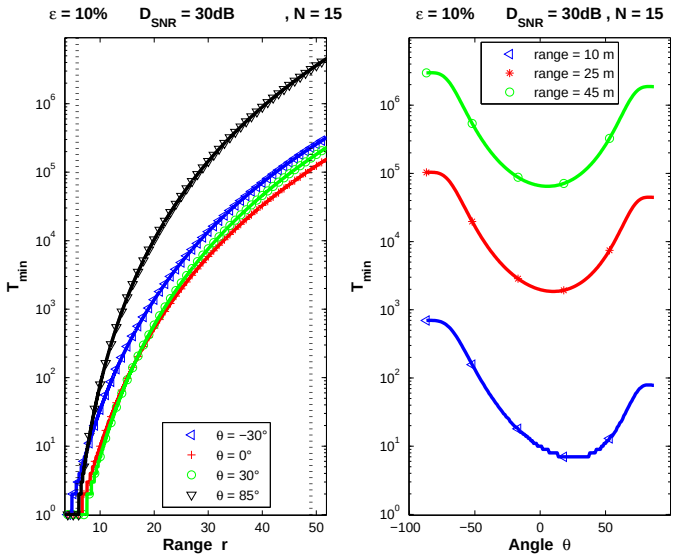

Fig. 9. Variation of the minimum observation time versus the source location parameters

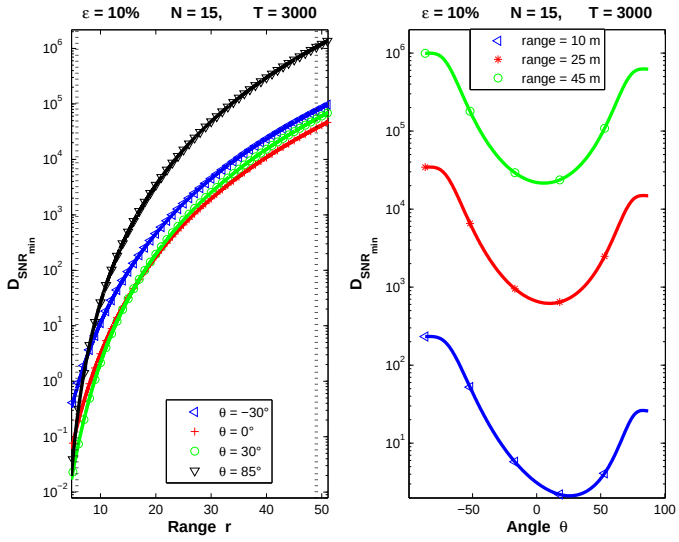

Fig. 10. Variation of the minimum deterministic SNR versus the source location parameters

APPENDIX A

PROOF OF LEMMA 1

A direct calculation of matrix $\boldsymbol{Q}$ in (17) using equation (16) leads to

$$\boldsymbol{Q} = \begin{pmatrix} \mathbf{Q}_1 & \mathbf{Q}_2^T \\ \mathbf{Q}_2 & \mathbf{Q}_3 \end{pmatrix}, \tag{82}$$

where

$$\mathbf{Q}_1 = \begin{pmatrix} f_{\theta\theta} & f_{\theta r} \\ f_{r\theta} & f_{rr} \end{pmatrix}, \quad \mathbf{Q}_2 = \begin{pmatrix} \mathbf{v}_1 & \mathbf{v}_1' \\ \mathbf{v}_2 & \mathbf{v}_2' \end{pmatrix}, \quad \mathbf{Q}_3 = \begin{pmatrix} v_3 \ \text{diag}(\boldsymbol{\alpha} \odot \boldsymbol{\alpha}) & \mathbf{0}_{T\times T} \\ \mathbf{0}_{T\times T} & v_3 \mathbf{I}_{T\times T} \end{pmatrix}.$$

The entries of $\mathbf{Q}_1$ are given by (19), (20) and (21), $\mathbf{v}_1 = \frac{2}{\sigma^2}(\boldsymbol{\gamma} \odot \boldsymbol{\gamma})^T \dot{\boldsymbol{\tau}}_\theta (\boldsymbol{\alpha} \odot \boldsymbol{\alpha})$, $\mathbf{v}_2 = \frac{2}{\sigma^2}(\boldsymbol{\gamma}^T \dot{\boldsymbol{\gamma}}_\theta)\boldsymbol{\alpha}$, $\mathbf{v}_1' = \frac{2}{\sigma^2}(\boldsymbol{\gamma} \odot \boldsymbol{\gamma})^T \dot{\boldsymbol{\tau}}_r (\boldsymbol{\alpha} \odot \boldsymbol{\alpha})$, $\mathbf{v}_2' = \frac{2}{\sigma^2}(\boldsymbol{\gamma}^T \dot{\boldsymbol{\gamma}}_r)\boldsymbol{\alpha}$, and $v_3 = \frac{2}{\sigma^2}\|\boldsymbol{\gamma}\|^2$.

Because the CRB of the range and the angle parameters is equal to the 2×2 top left sub-matrix of the inverse matrix $\boldsymbol{Q}^{-1}$, Schur lemma [26] can be used and the results will be as $\boldsymbol{Q}^{-1} = \begin{pmatrix} \mathbf{Q}_c^{-1} & \mathbf{x} \\ \mathbf{x} & \mathbf{x} \end{pmatrix}$ where $\mathbf{Q}_c = \mathbf{Q}_1 - \mathbf{Q}_2^T.\mathbf{Q}_3^{-1}.\mathbf{Q}_2$.

After a straightforward computation, one obtain

$$\mathbf{Q}_c = \begin{pmatrix} f_{\theta\theta} - \frac{1}{v_3}(\mathbf{v}_1^T(\text{diag}(\boldsymbol{\alpha} \odot \boldsymbol{\alpha}))^{-1}\mathbf{v}_1 + \mathbf{v}_2^T\mathbf{v}_2) & f_{\theta r} - \frac{1}{v_3}(\mathbf{v}_1^T(\text{diag}(\boldsymbol{\alpha} \odot \boldsymbol{\alpha}))^{-1}\mathbf{v}_1' + \mathbf{v}_2^T\mathbf{v}_2') \\ f_{r\theta} - \frac{1}{v_3}(\mathbf{v}_1'^T(\text{diag}(\boldsymbol{\alpha} \odot \boldsymbol{\alpha}))^{-1}\mathbf{v}_1 + \mathbf{v}_2'^T\mathbf{v}_2) & f_{rr} - \frac{1}{v_3}(\mathbf{v}_1'^T(\text{diag}(\boldsymbol{\alpha} \odot \boldsymbol{\alpha}))^{-1}\mathbf{v}_1' + \mathbf{v}_2'^T\mathbf{v}_2') \end{pmatrix}, \tag{83}$$

where $(\text{diag}(\boldsymbol{\alpha} \odot \boldsymbol{\alpha}))^{-1}$ refers to the inverse of the diagonal matrix $\text{diag}(\boldsymbol{\alpha} \odot \boldsymbol{\alpha})$ formed from vector $\boldsymbol{\alpha} \odot \boldsymbol{\alpha}$.

Now, by comparing this expression of $\mathbf{Q}_c$ to the expressions in (36), (37) and (38), one can rewrite

$$\mathbf{Q}_c = 2TD_{\text{SNR}} \begin{pmatrix} E_{vg}(\theta) & -E_{vg}(\theta, r) \\ -E_{vg}(r, \theta) & E_{vg}(r) \end{pmatrix}, \tag{84}$$

leading finally to

$$\text{VG-CRB}^c(\theta) = \frac{E_{vg}(r)}{\det(\mathbf{Q}_c)} = \left(\frac{1}{2TD_{\text{SNR}}}\right) \frac{E_{vg}(r)}{E_{vg}(\theta)E_{vg}(r) - E_{vg}(\theta, r)^2}, \tag{85}$$

$$\text{VG-CRB}^c(r) = \frac{E_{vg}(\theta)}{\det(\mathbf{Q}_c)} = \left(\frac{1}{2TD_{\text{SNR}}}\right) \frac{E_{vg}(\theta)}{E_{vg}(\theta)E_{vg}(r) - E_{vg}(\theta, r)^2}, \tag{86}$$

$$\text{VG-CRB}^c(\theta, r) = \frac{E_{vg}(\theta, r)}{\det(\mathbf{Q}_c)} = \left(\frac{1}{2TD_{\text{SNR}}}\right) \frac{E_{vg}(\theta, r)}{E_{vg}(\theta)E_{vg}(r) - E_{vg}(\theta, r)^2}. \tag{87}$$

APPENDIX B
PROOF OF LEMMA 2

For the unconditional case, the considered unknown parameter vector is $\boldsymbol{\xi}^u = (\theta, r, \sigma_s^2, \sigma^2)^T$ which leads to the following 4×4 Fisher Information matrix FIM $= \begin{pmatrix} \mathbf{F}_1 & \mathbf{F}_2 \\ \mathbf{F}_2^T & \mathbf{F}_3 \end{pmatrix}$ where the 2×2 matrices $\mathbf{F}_i$ are given by

$$\mathbf{F}_1 = \begin{pmatrix} f_{\theta\theta} & f_{\theta r} \\ f_{r\theta} & f_{rr} \end{pmatrix}, \quad \mathbf{F}_2 = \begin{pmatrix} f_{\theta\sigma_s^2} & f_{\theta\sigma^2} \\ f_{r\sigma_s^2} & f_{r\sigma^2} \end{pmatrix}, \quad \mathbf{F}_3 = \begin{pmatrix} f_{\sigma_s^2\sigma_s^2} & f_{\sigma_s^2\sigma^2} \\ f_{\sigma^2\sigma_s^2} & f_{\sigma^2\sigma^2} \end{pmatrix}.$$

By using Schur's lemma for matrix inversion [26], one can obtain FIM$^{-1} = \begin{pmatrix} \mathbf{L}^{-1} & \mathbf{G} \\ \mathbf{G}^T & \mathbf{H} \end{pmatrix}$. where $\mathbf{L} = \mathbf{F}_1 - \mathbf{F}_2\mathbf{F}_3^{-1}\mathbf{F}_2^T = \begin{pmatrix} u & x \\ x & v \end{pmatrix}$. $\mathbf{F}_3$ and $\mathbf{L}$ are 2×2 matrices and their inverse can be computed easily as

$$\mathbf{L}^{-1} = \frac{1}{\det} \begin{pmatrix} u & -x \\ -x & v \end{pmatrix} = \begin{pmatrix} \text{CRB}(r) & \text{CRB}(\theta, r) \\ \text{CRB}(\theta, r) & \text{CRB}(\theta) \end{pmatrix}, \tag{88}$$

where

$$u = f_{rr} - \frac{1}{\det_1}(f_{\theta\sigma_s^2}c_1 + f_{\theta\sigma^2}c_2), \tag{89}$$

$$v = f_{\theta\theta} - \frac{1}{\det_1}(f_{r\sigma_s^2}c_1 + f_{r\sigma^2}c_2), \tag{90}$$

$$x = f_{r\theta} - \frac{1}{\det_1}(f_{r\sigma_s^2}c_3 + f_{r\sigma^2}c_4), \tag{91}$$

$$\det_1 = f_{\sigma^2\sigma^2}f_{\sigma_s^2\theta} - f_{\sigma_s^2\sigma^2}f_{\sigma^2\theta}, \tag{92}$$

$$c_1 = f_{\sigma^2\sigma^2}f_{\sigma_s^2\theta} - f_{\sigma_s^2\sigma^2}f_{\sigma^2\theta}, \tag{93}$$

$$c_2 = f_{\sigma_s^2\sigma_s^2}f_{\sigma^2\theta} - f_{\sigma^2\sigma_s^2}f_{\sigma_s^2\theta}, \tag{94}$$

$$c_3 = f_{\sigma_s^2\sigma_s^2}f_{\sigma_s^2 r} - f_{\sigma_s^2\sigma^2}f_{\sigma^2 r}, \tag{95}$$

$$c_4 = f_{\sigma_s^2\sigma_s^2}f_{\sigma^2 r} - f_{\sigma^2\sigma_s^2}f_{\sigma_s^2 r}, \tag{96}$$

$$\det = uv - x^2. \tag{97}$$

Now, it remains only to compute the entries of the FIM by using equation (40) and taking into account that the matrix $\mathbf{\Sigma} = \sigma_s^2 \boldsymbol{a}(\theta, r)\boldsymbol{a}(\theta, r)^H + \sigma^2 \mathbf{I}_N$ and its inverse is given as $\mathbf{\Sigma}^{-1} = \frac{1}{\sigma^2}(\mathbf{I}_N - \frac{1}{C}\boldsymbol{a}(\theta, r)\boldsymbol{a}(\theta, r)^H)$ where $C = \frac{1}{\text{SNR}} + \|\boldsymbol{\gamma}\|^2$ and $\boldsymbol{a}(\theta, r) = [\gamma_0, \gamma_1 e^{j\tau_1}, \cdots, \gamma_{N-1} e^{j\tau_{N-1}}]^T$.

A straightforward (but cumbersome) computation leads to

$$
\begin{aligned}
f_{\theta\theta} &= \frac{2T}{C^2}(1 - \text{SNR}\,\|\boldsymbol{\gamma}\|^2) - (1 + \text{SNR}\,\|\boldsymbol{\gamma}\|^2)((\boldsymbol{\gamma} \odot \boldsymbol{\gamma})^T \dot{\boldsymbol{\tau}}_\theta)^2 && (98)\\
&\quad + C\ \text{SNR}\,\|\boldsymbol{\gamma}\|^2 (\|\dot{\boldsymbol{\gamma}}_\theta\|^2 + (\boldsymbol{\gamma} \odot \boldsymbol{\gamma})^T (\dot{\boldsymbol{\tau}}_\theta \odot \dot{\boldsymbol{\tau}}_\theta)),\\
f_{rr} &= \frac{2T}{C^2}(1 - \text{SNR}\,\|\boldsymbol{\gamma}\|^2)(\boldsymbol{\gamma}^T \dot{\boldsymbol{\gamma}}_r)^2 - (1 + \text{SNR}\,\|\boldsymbol{\gamma}\|^2)((\boldsymbol{\gamma} \odot \boldsymbol{\gamma})^T \dot{\boldsymbol{\tau}}_r)^2 && (99)\\
&\quad + C\ \text{SNR}\,\|\boldsymbol{\gamma}\|^2 (\|\dot{\boldsymbol{\gamma}}_r\|^2 + (\boldsymbol{\gamma} \odot \boldsymbol{\gamma})^T (\dot{\boldsymbol{\tau}}_r \odot \dot{\boldsymbol{\tau}}_r)),\\
f_{r\theta} &= \frac{2T}{C^2}(1 - \text{SNR}\,\|\boldsymbol{\gamma}\|^2)(\boldsymbol{\gamma}^T \dot{\boldsymbol{\gamma}}_\theta)(\boldsymbol{\gamma}^T \dot{\boldsymbol{\gamma}}_r) - (1 + \text{SNR}\,\|\boldsymbol{\gamma}\|^2)((\boldsymbol{\gamma} \odot \boldsymbol{\gamma})^T \dot{\boldsymbol{\tau}}_\theta)((\boldsymbol{\gamma} \odot \boldsymbol{\gamma})^T \dot{\boldsymbol{\tau}}_r)\\
&\quad + C\ \text{SNR}\,\|\boldsymbol{\gamma}\|^2 (\dot{\boldsymbol{\gamma}}_\theta^T \dot{\boldsymbol{\gamma}}_r + (\boldsymbol{\gamma} \odot \boldsymbol{\gamma})^T (\dot{\boldsymbol{\tau}}_\theta \odot \dot{\boldsymbol{\tau}}_r)), && (100)\\
f_{\sigma_s^2\sigma_s^2} &= \frac{T\,\|\boldsymbol{\gamma}\|^4}{\sigma^4 (C\ \text{SNR})^2}, && (101)\\
f_{\sigma^2\sigma^2} &= \frac{T}{\sigma^4 C^2}(NC^2 - \|\boldsymbol{\gamma}\|^2 (2C - \|\boldsymbol{\gamma}\|^2)), && (102)\\
f_{\sigma_s^2\sigma^2} &= \frac{T\,\|\boldsymbol{\gamma}\|^4}{\sigma^4 (C\ \text{SNR})^2}, && (103)\\
f_{\theta\sigma_s^2} &= \frac{2T\,\|\boldsymbol{\gamma}\|^2}{\sigma^2 C^2 \text{SNR}}(\boldsymbol{\gamma}^T \dot{\boldsymbol{\gamma}}_\theta), && (104)\\
f_{\theta\sigma^2} &= \frac{2T}{\sigma^2 C^2 \text{SNR}}(\boldsymbol{\gamma}^T \dot{\boldsymbol{\gamma}}_\theta), && (105)\\
f_{r\sigma_s^2} &= \frac{2T\,\|\boldsymbol{\gamma}\|^2}{\sigma^2 C^2 \text{SNR}}(\boldsymbol{\gamma}^T \dot{\boldsymbol{\gamma}}_r), && (106)\\
f_{r\sigma^2} &= \frac{2T}{\sigma^2 C^2 \text{SNR}}(\boldsymbol{\gamma}^T \dot{\boldsymbol{\gamma}}_r). && (107)
\end{aligned}
$$

By replacing these entries in equations (89)-(97), we obtain

$$
\begin{aligned}
u &= \frac{2T\text{SNR}^2\,\|\boldsymbol{\gamma}\|^2}{(1 + \text{SNR}\,\|\boldsymbol{\gamma}\|^2)} E_{vg}(r), && (108)\\
v &= \frac{2T\text{SNR}^2\,\|\boldsymbol{\gamma}\|^2}{(1 + \text{SNR}\,\|\boldsymbol{\gamma}\|^2)} E_{vg}(\theta), && (109)\\
x &= \frac{2T\text{SNR}^2\,\|\boldsymbol{\gamma}\|^2}{(1 + \text{SNR}\,\|\boldsymbol{\gamma}\|^2)} E_{vg}(\theta, r), && (110)
\end{aligned}
$$

leading finally to Lemma 2 result

$$\text{VG-CRB}^u(\theta) = \frac{1+\text{SNR}\left\|\boldsymbol{\gamma}\right\|^2}{2T\text{SNR}^2\left\|\boldsymbol{\gamma}\right\|^2}\frac{E_{vg}(r)}{E_{vg}(\theta)E_{vg}(r)-E_{vg}(\theta,r)^2}, \quad (111)$$

$$\text{VG-CRB}^u(r) = \frac{1+\text{SNR}\left\|\boldsymbol{\gamma}\right\|^2}{2T\text{SNR}^2\left\|\boldsymbol{\gamma}\right\|^2}\frac{E_{vg}(\theta)}{E_{vg}(\theta)E_{vg}(r)-E_{vg}(\theta,r)^2}, \quad (112)$$

$$\text{VG-CRB}^u(r,\theta) = \frac{1+\text{SNR}\left\|\boldsymbol{\gamma}\right\|^2}{2T\text{SNR}^2\left\|\boldsymbol{\gamma}\right\|^2}\frac{E_{vg}(\theta,r)}{E_{vg}(\theta)E_{vg}(r)-E_{vg}(\theta,r)^2}. \quad (113)$$

REFERENCES

[1] H. Krim, M. Viberg, "Two decades of array signal processing research: The parametric approach," *IEEE Signal Processing Magazine*, vol. 13, pp. 67–94, July 1996.

[2] S. Asgari, *Far-field DOA estimation and source localization for different scenarios in a distributed sensor network*, PhD Thesis, UCLA, 2008.

[3] A.J. Weiss, B. Friedlander, "Range and bearing estimation using polynomial rooting," *IEEE Journal of Oceanic Engineering*, vol. 18, pp. 130–137, April 1993.

[4] A.L. Swindlehurst, T. Kailath, "Passive direction-of-arrival and range estimation for near-field sources," *In Proceedings: Annual ASSP Workshop on Spectrum Estimation and Modeling*, pp. 123 – 128, August 1988.

[5] G. Arslan, F.A. Sakarya, "Unified neural-network-based speaker localization technique," *IEEE Transactions on Neural Networks*, vol. 11, pp. 997 – 1002, July 2000.

[6] F. Asono, H. Asoh, T. Matsui, "Sound source localization and signal separation for office robot JiJo-2," *In Proceedings: Multisensor Fusion and Integration for Intelligent Systems conference (MFI)*, pp. 243 – 248, August 1999.

[7] P. Tichavsky, K.T. Wong, M.D. Zoltowski, "Near-field/far-field azimuth and elevation angle estimation using a single vector-hydrophone," *IEEE Transactions on Signal Processing*, vol. 49, pp. 2498 – 2510, November 2001.

[8] C.H. Schmidt, T.F. Eibert, "Assessment of irregular sampling near-field far-field transformation employing plane-wave field representation," *IEEE Antennas and Propagation Magazine*, vol. 53, pp. 213 – 219, June 2011.

[9] T. Vaupel, T.F. Eibert, "Comparison and application of near-field ISAR imaging techniques for far-field radar cross section determination," *IEEE Transactions on Antennas and Propagation*, vol. 54, pp. 144 – 151, January 2006.

[10] N.L. Owsley, "Array phonocardiography," *In Proceedings: Adaptive Systems for Signal Processing, Communications, and Control Symposium (AS-SPCC)*, pp. 31 – 36, October 2000.

[11] J. He, M.N.S. Swamy, M.O. Ahmad, "Efficient application of MUSIC algorithm under the coexistence of far-field and near-field sources," *IEEE Transactions on Signal Processing*, vol. 60, pp. 2066–2070, April 2012.

[12] Junli Liang, Ding Liu, "Passive localization of mixed near-field and far-field sources using two-stage music algorithm," *IEEE Transactions on Signal Processing*, vol. 58, pp. 108–120, January 2010.

[13] E. Grosicki, K. Abed-Meraim, Hua Yingbo , "A weighted linear prediction method for near-field source localization," *IEEE Transactions on Signal Processing*, vol. 53, pp. 3651–3660, October 2005.

[14] L. Kopp, D. Thubert, "Bornes de Cramér-Rao en traitement d'antenne, première partie : Formalisme," *Traitement du Signal*, vol. 3, pp. 111–125, 1986.

[15] M.N. El Korso, R. Boyer, A. Renaux, S. Marcos, "Conditional and unconditional Cramér Rao Bounds for near-field source localization," *IEEE Transactions on Signal Processing*, vol. 58, pp. 2901–2907, May 2010.

[16] Y. Begriche, M. Thameri, K. Abed-Meraim, "Exact Cramer Rao Bound for near field source localization ," *11th International Conference on Information Science, Signal Processing and their Applications (ISSPA)*, pp. 718 – 721, July 2012.

[17] C.A. Balanis, *Antenna theory: Analysis and design*, Third edition, Wiley Interscience, 2005.

[18] S. Park, E. Serpedin, K. Qaraqe, "Gaussian assumption: The least favorable but the most useful," *IEEE Signal Processing Magazine*, pp. 183–186, May 2013.

[19] P. Stoica, R.L. Moses , *Introduction to Spectral Analysis*, Prentice Hall, 1997.

[20] D. Rahamim, J. Tabrikian, R. Shavit, "Source localization using vector sensor array in a multipath environment," *IEEE Transactions on Signal Processing*, vol. 52, pp. 3096–3103, Nouvember 2004.

[21] E. Grosicki, K. Abed-Meraim, Y. Hua, "A weighted linear prediction method for near-field source localization," *IEEE Transactions on Signal Processing*, vol. 53, pp. 3651 – 3660, October 2005.

[22] P. Stoica, E.G. Larsson, A.B. Gershman, "The stochastic CRB for array processing: a textbook derivation," *IEEE Signal Processing Letters*, vol. 8, pp. 148 – 150, May 2001.

[23] Axel Kpper, *Location-Based Services: Fundamentals and Operation*, John Wiley and sons, Ltd, 2005.

[24] "RTCA Minimum Operational Performance Standards for Global Positioning System/Wide Area Augmentation System Airborne Equipment. 1828 L Street, NW Suite 805, Washington, D.C. 20036 USA," .

[25] G. Casella, R.L. Berger, *Statistical inference*, Second edition, Duxbury Press, 2001.

[26] W.H. Press, S.A. Teukolsky, W.T. Vetterling, B.P. Flannery, *Numerical recipes: The art of scientific computing*, Third Edition, Cambridge University Press, 2007.